IET Intelligent Transport Systems

WILEY

IET The Institution of Engineering and Technology

ORIGINAL RESEARCH OPEN ACCESS

A Stochastic Geometry Framework for Enhancing Communication Efficiency and Road Safety in Connected and Autonomous Vehicles

Anjum Mohd Aslam[1] | Aditya Bhardwaj[2] | Xiaochun Cheng[3]

[1]Department of CSE, Sharda School of Computing Science & Engineering (SSCSE), Sharda University, Greater Noida, U.P., India | [2]SCSET, Bennett University, Greater Noida, U.P., India | [3]Computer Science Department, Swansea University, Bay Campus, Swansea University, Wales, UK

Correspondence: Anjum Mohd Aslam (anjum12021@gmail.com) | Aditya Bhardwaj (aditya.cse@nitttrchd.ac.in) | Xiaochun Cheng (xiaochun.cheng@swansea.ac.uk)

Received: 1 June 2025 | **Revised:** 12 February 2026 | **Accepted:** 8 March 2026

ABSTRACT

Connected and autonomous vehicles (CAVs) are critical to the advancement of intelligent transportation systems (ITS) and the realisation of completely autonomous driving. CAVs' sophisticated technologies enable the seamless transmission of essential information in real-time, promoting greater road safety and efficient transportation networks. However, due to the complex and time-sensitive nature of information transmission between vehicles and infrastructure units, developing reliable and efficient wireless communication networks for CAVs poses major challenges. It is critical to effectively deploy connected and autonomous driving technologies to ensure seamless and reliable communication between CAVs and the surrounding infrastructure. In this paper, we designed an effective mathematical approach for evaluating the performance of vehicular communication networks based on stochastic geometry principles. The architecture of a dynamic CAVs scenario is illustrated by modelling the spatial layout of pathways with the Poisson line process (PLP) and the positioning of CAVs and infrastructure units on each path with the Poisson point process (PPP). By deriving expressions for key metrics such as signal-to-interference-plus-noise ratio (SINR), spatial coverage, and link success probability under Nakagami-m fading, the framework offers deep insights into the reliability and efficiency of vehicle-to-everything (V2X) communications. The simulation results give valuable insights for designing and implementing CAVS, with stochastic geometry leading to improved overall CAVs performance.

1 | Introduction

Recent advances in information and communication technology have given rise to intelligent transportation systems (ITS) as a transformative technology, revolutionizing transportation by offering safer and more efficient driving experiences [1]. Over the past decades, the automotive sectors have diligently worked to improve advanced driver-assistance systems (ADAS) and pave the way for the deployment of fully autonomous vehicles that are capable of driving without human assistance. At the forefront of this evolution are connected and autonomous vehicles (CAVs), a key concept driving the future of transportation that aims to provide greater mobility and enhanced road safety [2]. CAVs integrate various technologies and are envisioned to provide enhanced transportation efficiency, minimized environmental impact, reduced accidents, improved safety, and diverse mobility service options [3]. The growing demand for CAVs is driven by a wide range of applications including road safety support, emergency alert notifications, blind spot warnings, traffic management, automatic parking assistance, and full automation. It is widely expected that the CAVs will continue to steadily unfold and progress throughout the 2020s and 2030s, with significant

advancements in infrastructure and communication technologies [4]. As the global CAV market continues to expand, it is anticipated to become one of the most significant marketplaces worldwide, estimated to reach a staggering $7 trillion by the year 2050 [5].

Vehicular communications networks play a pivotal role in enabling seamless communication among CAVs and other infrastructural units, such as roadside units (RSUs). This communication occurs in real-time through vehicle-to-vehicle (V2V) and vehicle-to-infrastructure (V2I) communications, thus forming a comprehensive vehicle-to-everything (V2X) communication ecosystem. CAVs actively share their trajectories and exchange critical information with each other and with infrastructural units, thereby, facilitating collective intelligence and informed decision-making for efficient traffic management [6]. However, despite promising advancements in CAV technology, substantial challenges persist to ensure safety and reliability in dense traffic scenarios. The increasing density of traffic has led to interference issues and limitations in data transmission coverage. The increasing complexity of urban areas adds further uncertainty and demands more sophisticated autonomous CAVs deployments. Moreover, the shared spectrum use and the inevitable geometry of road traffic scenarios pose potential challenges in terms of vehicle-to-vehicle radar interference [7].

Furthermore, the rising worldwide interest in ITS to enhance transportation efficiency and safety has led to a growing research focus on connected and autonomous vehicles (CAV). According to the US Census Bureau report, there are approximately 10 million road accidents that occur annually in the US, with an average fatality rate of 1.5% [8]. The Federal Highway Administration (FHA) estimates that 40% of all accidents occur annually at intersections, encompassing fatalities, injuries, and property damage crashes [9]. In wireless urban networks, high user density, numerous buildings, and unpredictable obstacles result in excessive interference and scattering issues, significantly impacting the overall driving experience. CAVs offers diverse applications to prevent accidents and improve safety in close proximity. However, interference from other transmitting vehicles is a crucial limitation affecting its performance in terms of outage probability. Hence, it is essential to address interference dependence when designing safety applications and protocols, especially at urban and suburban intersections.

Several studies have been conducted in the literature to analyze CAVs using the principles of stochastic geometry, aiming to balance the tradeoff between the success probability and other performance metrics. The authors in [8] developed an analytical framework using stochastic geometry to model CSMA-coordinated multi-hop inter-vehicle communication on highways to maximize the aggregate packet progress to enable efficient data transmission. The theoretical and statistical studies presented in [7, 10] characterize the baseband aggregate interference, outage probability, and transmission rate analysis in cellular networks, focusing on the implementation of interference protection mechanisms around receivers. Safety message dissemination in vehicular communication poses significant challenges, necessitating vehicle-to-vehicle (V2V) communication with low latency and high reliability. To meet these stringent requirements, the authors in [11] proposed a geolocation-based access (GLOC) approach for direct V2V communication. The GLOC scheme aims to maximize the distance between co-channel transmitters while ensuring low latency resource access and minimal overhead. To analyze the performance of various resource selection schemes in cellular vehicle-to-everything (C-V2X), the control information-assisted three-step (CIAT) resource selection process is modeled and analyzed using the tools of Poisson process theory in [2]. The model takes into account the distribution of interfering vehicles and provides valuable analytical insights into important metrics such as the resource exclusion ratio, average successful transmission probability, and packet inter-reception time in vehicular communication networks.

Despite these significant contributions, existing PLP/PPP-based studies either focus on highway-centric scenarios, protocol-specific designs, or general cellular abstractions. They do not jointly characterize the spatial coverage and link success probability of an arbitrary receiver under realistic road topology, traffic density, and fading conditions. In particular, the system-level reliability analysis of a tagged receiver connecting to its nearest transmitter in a PLP-based road network remains insufficiently explored. In this paper, we aim to address these challenges and contribute to the development of ITS by leveraging cutting-edge technologies, including sensor technologies and wireless communications. We design an analytical framework for modeling vehicular communication networks, utilizing the principles of stochastic geometry and Poisson process theory. Rather than proposing a new MAC or resource allocation scheme, our approach provides a tractable system-level analysis that explicitly models road layouts using a Poisson line process (PLP). It derives closed-form expressions for SINR, spatial coverage, and link success probability under Nakagami-m fading. The proposed approach will assess the performance of CAV communications, considering crucial factors such as interference, link success probability, and traffic density network parameters.

1.1 | Contribution

The main contribution of our research study is summarized as follows:

- We present a robust analytical framework for modeling vehicular communication and analyzing the performance of V2X communications by integrating concepts from stochastic geometry. The framework models the complex spatial distribution and mobility patterns of vehicles using the Poisson point process theory, providing a realistic representation of real-world V2X scenarios.
- We present a methodology for computing the average signal-to-interference-plus-noise ratio (SINR) to estimate the link success probability of an arbitrary receiver connecting to the closest node. This enables the evaluation of the communication reliability of CAVs, thereby contributing to the design of more robust and efficient communication protocols for improved transportation efficiency.
- Consequently, we analyze the impact of critical network parameters, such as node density and path density, on the link success probability. This study investigates how the variations in these parameters affect the likelihood of successful trans-

mission, thereby providing practical insights for optimizing communication infrastructure. By analyzing these factors, we provide a more comprehensive overview of the trade-offs between road safety and communication performance, with our framework enabling both effective vehicle communication and improving road safety in real-world CAV deployments.

The remainder of the paper is organized as follows. Section 2 presents related work. Further, in Section 3, we present the stochastic geometry preliminaries used to model the CAVs. Section 4 describes the network system model. In Section 5, we define the methodological approach for categorizing interference. We derive the expression for SINR for an arbitrary receiver and subsequently compute the expression for the probability of successful transmission. Section 6 presents the simulation setup and performance evaluation results in Section 7. Finally, in Section 8, we summarize our contributions.

2 | Related Work

The advancement of CAVs has driven significant research in optimizing communication efficiency and road safety. Various techniques and models have been proposed to address key challenges, such as efficient lane merging, trajectory prediction, cooperative decision-making, and vehicular communication. Among these, game-theoretic approaches have received substantial attention due to their capacity to model the interactions between CAVs and other human-driven vehicles (HVs) in mixed traffic scenarios [12]. Normalized cooperative level-k (NCL) game and multi-lane merging coalition game are prime examples of such approaches [13]. The NCL model integrates cooperative behavior with level-k reasoning, which enables optimal decision-making for collision-free trajectories [14]. On the other hand, the coalition game framework facilitates cooperative merging decisions among CAVs on multi-lane highways. Despite their promise, these models face computational complexity challenges, especially in large-scale multi-agent systems, and are limited by the presence of human-driven vehicles in mixed-traffic environments.

Another line of research focuses on stochastic geometry-based models for vehicular communication. These models aim to improve link reliability and message propagation efficiency in V2V and vehicle-to-infrastructure (V2I) communication. The stochastic geometry for inter-vehicle communication model applies stochastic geometry to model V2V message dissemination under different traffic conditions [15]. Similarly, the stochastic roadside unit (RSU) location optimization approach aims to optimize the placement of RSUs to improve information propagation and reduce deployment costs. Stochastic geometry for automotive radar models radar interference, allowing for more accurate radar-based object detection in dense traffic environments. In this study, our proposed stochastic geometry framework for CAVs extends these concepts by utilizing a combination of the PLP and Poisson point process (PPP) to model road layouts and vehicle locations. This model provides a novel way to evaluate SINR, link success probability, and spatial coverage in CAV networks.

Further, deep learning techniques have also been adopted in literature to address trajectory prediction and control challenges for CAVs [16, 17]. The cognition-inspired trajectory prediction approach stands out in this domain. By integrating convolutional neural networks (CNNs) and graph attention networks (GATs), this model leverages the cognitive characteristics of human drivers to predict future vehicle trajectories more accurately. This approach outperforms traditional trajectory prediction methods, especially in interactive scenarios like intersections and roundabouts, where human-like decision-making plays a crucial role. However, such models rely heavily on large datasets for training and face limitations in generalizing across unseen traffic scenarios. Moreover, level-K reasoning with deep reinforcement learning (DRL) and Monte Carlo tree search (MCTS) incorporate game theory with DRL to enable fast and safe lane changes, providing robust solutions in rapidly changing environments [14]. These models are more adaptive but computationally intensive, especially when deployed in real-time traffic scenarios with multiple agents.

Finally, cooperative communication models for intersections have been extensively explored to enhance road safety and efficiency. The decode-and-forward relay at intersections scheme considers hybrid transmission schemes for V2V and V2I communication under Nakagami-m fading channels [18]. By employing a combination of direct transmission, relay transmission, and hybrid transmission, the model achieves high transmission reliability, especially in scenarios where direct communication is obstructed. Another example is the non-cooperative game-based shared steering control model, which utilizes non-cooperative game theory to balance human-driven and autonomous vehicle steering control [19]. This approach enhances driver-centric automation but requires careful tuning of driver adaptability and system responses. Table 1 presents the key characteristics and provides a comparative analysis of the existing approaches.

In summary, the literature on CAVs communication efficiency and road safety reveals a growing interest in game-theoretic models, stochastic geometry-based approaches, and deep learning-driven trajectory prediction. The integration of these techniques into unified models, such as the proposed stochastic geometry framework for CAVs, offers promising directions for enhancing V2X communications, reducing interference, and ensuring safe lane changes and merging. While these approaches have demonstrated effectiveness in simulations, real-world deployment requires further refinement, particularly in addressing computational overheads, adaptability to mixed traffic environments, and real-time decision-making under uncertainty.

3 | Stochastic Geometry Preliminaries

Stochastic geometry is a branch of probability theory [24], that focuses on the study of random spatial patterns and structures in Euclidean space. It has emerged as a powerful optimization tool for modeling and analysis of wireless networks [8]. The main aim of the stochastic optimization model is to anticipate and regulate various performance metrics in the network, including the analysis of mutual interference between transceivers, SINR, and outage probability [10]. Stochastic geometry utilizes point process theory [25], an essential component of stochastic modeling to effectively model and analyze optimization problems that incorporate uncertainty in wireless networks. By leveraging

TABLE 1 | Comparative summary of existing relevant related work.

Author	Year	Approach applied	Contribution	Limitations
Baha et al. [18]	2019	Cooperative communications, Nakagami-m fading.	Uses hybrid transmission (direct, relay, and hybrid) schemes for V2V and V2I communication at intersections.	Performance depends on LOS/NLOS conditions, and optimal relay positioning can be challenging in dynamic traffic.
Yunyi et al. [20]	2021	Stochastic programming.	Uses two-stage mixed-integer nonlinear stochastic programming to optimize RSU locations for multihop information propagation.	Relies on accurate traffic density estimates, and cost of RSU deployment may be high in large areas.
Tengchan et al. [16]	2022	Federated learning (FL) for CAV controller design.	Proposes a FL framework using a dynamic federated proximal (DFP) algorithm to collaboratively optimize autonomous controller design, ensuring robust operation under varying road and wireless conditions.	Performance depends on CAV participation and data quality; wireless fading and mobility may impact FL convergence.
Kyoungtae et al. [21]	2023	Hierarchical game-theoretic approach for V2X communications.	Combines hierarchical decision-making with game theory for CAV overtaking scenarios using V2X information.	High computational cost due to global and local aggressiveness estimation and high dependency on V2X data.
Minghao et al. [22]	2023	Coalition game theory.	Multi-CAV cooperative decision-making using coalition game theory, handling CAV-CMV interactions and perceived risks.	High computational complexity, especially with an increasing number of interacting vehicles in mixed traffic.
Ziye et al. [12]	2024	Multi-agent game-theory.	Applies game-theoretic models for managing CAV-Human-driven Vehicles (HV) interactions, focusing on cooperation and efficiency at intersections.	Complexity increases with multi-agent interactions, and driver non-compliance can disrupt efficiency.
Anjum et al. [23]	2024	Cooperative game-theoretic approach for multi-lane merging.	Proposes cooperative decision-making for CAVs to achieve safe and efficient multi-lane merging.	Requires precise knowledge of the intent and dynamics of other vehicles in real time.
Junhui et al. [19]	2024	Non-cooperative game for shared control.	Employs non-cooperative game theory for shared driver-automation steering control to ensure human-centric automation.	Driver adaptability is required, and performance may degrade if the driver exhibits erratic steering behavior.
Fang et al. [13]	2024	Normalized cooperative level-k (NCL) game.	Combines cooperative and level-k game theory for optimal and collision-free CAV trajectories at intersections.	Limited applicability in scenarios with low HV penetration, requires extensive computation for level estimation.
Proposed work	2025	Stochastic geometry (PLP-PPP), SINR-based analysis.	Provides an analytical framework for C-V2X networks by jointly modeling road topology using a Poisson Line Process and node distribution using 1D Poisson Point Processes.	Focuses on physical-layer reliability analysis; does not model protocol-specific MAC delays, scheduling mechanisms, or higher-layer control strategies.

its capabilities in CAVs, it can address the challenges posed by autonomous vehicles, such as optimizing connectivity, minimizing the interference due to signal collisions, and resource allocation for maximizing channel utilization, ultimately leading to improved network performance [15].

This section discusses the fundamental concepts of the PLP and point process theory, both of which hold significant importance in the realm of Stochastic geometry for modeling and analyzing V2X communications.

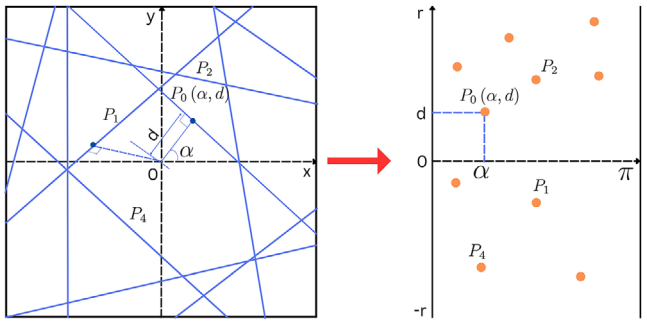

FIGURE 1 | Representation of the PLP in a two-dimensional plane ($\mathbb{R}^2$) alongside the corresponding PPP in the representation space $\mathcal{S} \equiv [0, \pi) \times \mathbb{R}$.

3.1 | PPP Essentials

Poisson point process is a prevalent mathematical model to describe the spatial distribution of points in a given region. CAVs have a distinctive spatial geometry, where the locations of vehicles on a road network are not uniformly distributed, exhibiting irregularity with no correlations in their positioning [7]. This spatial behavior can be effectively modeled using a homogeneous PPP denoted by $\psi = \{x_n\}$ with density ϱ over a two-dimensional plane ($\mathbb{R}^2$) in the representation space $\mathcal{S} \equiv [0, \pi) \times \mathbb{R}$ as shown in Figure 1.

The Poisson point process is characterized by the Poisson distribution, which expresses the likelihood of a random variable 'K', such that the probability of K = i is given by the following expression:

$$\mathbb{P}_r(K = i) = \frac{\gamma^i}{i!} e^{-\gamma} \tag{1}$$

where γ denotes the expected value of K. Thus, the PPP, which assumes the independent point locations, is the most commonly utilized point process in literature due to its simplicity and analytical tractability. It facilitates the study of spatial distribution and connectivity of CAVs and enables the analysis of coverage and connectivity in vehicular communication networks. By leveraging the PPP, CAVs can be optimized to improve overall system performance [26, 27].

3.2 | Poisson Line Process

CAVs possess distinctive spatial characteristics as vehicles are constrained to be positioned on roadways, forming a connected network, primarily following linear paths. To accurately represent and model these roadways, a line process can be employed, where the roadways are represented as a network of lines distributed across the plane using the PLP [28]. CAVs possess distinctive spatial characteristics as vehicles are constrained to be positioned on roadways, forming a connected network, primarily following linear paths. To accurately represent and model these roadways, a line process can be employed, where the roadways are represented as a network of lines distributed across the plane using the PLP [28]. This approach captures the random deployment of vehicles, while PLP models roadways to accurately represent the spatial structure of the CAV network. This modeling facilitates a realistic assessment of vehicular communication networks and assists in the derivation of important performance metrics, such as SINR and link success probability.

PLP is a random collection of lines in a two-dimensional plane, where each line in $\mathbb{R}^2$ is defined by its distance and angle from the origin. As illustrated in Figure 1, every undirected line P in $\mathbb{R}^2$ can be uniquely described by its perpendicular distance d and angle α. The polar coordinates (d, α) of the orthogonal projection of the origin O are characterized by $d \in \mathbb{R}$ and $\alpha \in [0, 2\pi]$. This transformation of a line P to a point (d, α) is referred to as the parametrization of the line. The coordinates (r, α) can be mapped as points in a half-cylinder C with a unit radius, defined as $C = [0, \pi] \times \mathbb{R}$. Thus, to ensure tractability, we assume that the points in C are represented by a PPP with the same density ϱ. Correspondingly, the process of lines in $\mathbb{R}^2$ forms a PLP with density ϱ. As depicted in Figure 1, for each line in the PLP Φ_l, there exists a corresponding point in the PPP, establishing a one-to-one correspondence between the two processes.

4 | System Model of CAVs

4.1 | Problem Formulation

The integration of V2X communications in ITS offers significant benefits, including improved data rates, spectrum efficiency, congestion alleviation, and reduced transmission latency. However, this integration also poses some challenges related to interference due to signal collision [29]. Today's automobiles are more connected than ever and use wireless communication for a variety of applications. Vehicular communications play a vital role in facilitating the exchange of safety-critical information, such as the locations of vehicles, speed, and obstacle alerts, between the vehicles and the infrastructure. This crucial information helps in improving road safety by proving timely warnings about potential collisions or accidents. However, this simultaneous transmission of signals from several vehicles that share the same time-frequency can lead to interference [18]. Such interference can significantly cause wireless networks to perform inadequately, impacting vehicular communications by reducing communication reliability.

Unlike the state-of-the-art models for PLP-PPP-based V2X communications, which mainly focus on highway-centric scenarios or generic cellular abstractions. The purpose of this research is to offer new system-level insight into the reliability of C-V2X communications from the viewpoint of an arbitrary tagged receiver with restrictions imposed by road geometry. Particularly, this model captures the effects of road topology (through a PLP), traffic density (through one-dimensional PPP), and wireless channel variability (through Nakagami-m fading) to provide an analytical formulation for interference, SINR, spatial coverage, and link success probability. The Nakagami-m fading model enables a flexible representation of real-world vehicular propagation environments. The smaller values of m correspond to severe multipath fading in dense urban areas, $m = 1$ reduces to Rayleigh fading, and larger values of $m > 1$ model milder fading conditions with a dominant line-of-sight component,

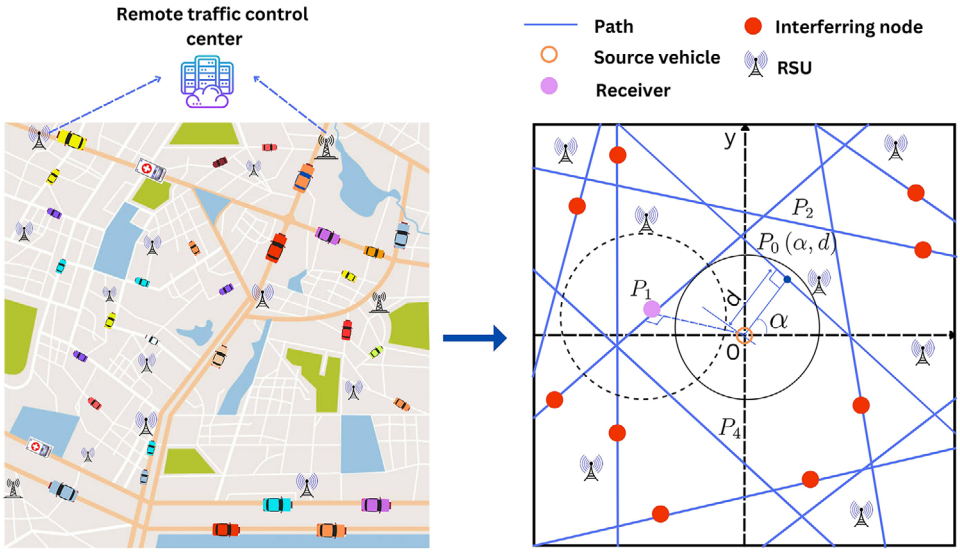

FIGURE 2 | An Illustration of seamless integration between dynamic CAVs scenario and stochastic geometry-based model.

which is prevalent in suburban and open-road deployments. The proposed analytical framework focuses on physical-layer interference and reliability characterization rather than protocol-specific medium access mechanisms. We emphasize that the proposed analysis targets an interference-limited C-V2X network, where aggregate co-channel interference is more dominant than thermal noise, and transmitting nodes are independently activated based on a thinning probability for analytical tractability. While IEEE 802.11p (DSRC) with CSMA is used in the simulation environment for numerical validation, the derived analytical expressions are equally applicable to sidelink-based LTE-V2X or NR-V2X systems under similar interference-limited conditions. Consequently, the framework provides a unified abstraction for studying SINR, spatial coverage, and link success probability across different V2X technologies without being tied to a specific MAC or scheduling protocol.

4.2 | Spatial Modeling of CAVs With Stochastic Geometry

Figure 2 provides a conceptual illustration of the proposed modeling approach. The left subfigure represents a realistic CAV deployment with physical road layouts, vehicles, and roadside units, while the right subfigure depicts the corresponding stochastic geometry abstraction used for analytical tractability. In the proposed framework, the road network is mapped to a PLP, and vehicles and infrastructure nodes located on each road are modeled using one-dimensional Poisson Point Processes (1D-PPPs).

For performance analysis, an arbitrary receiver (vehicle or infrastructure unit) is selected as the tagged receiver and placed at the origin without loss of generality using Slivnyak's theorem. The source vehicle is defined as the nearest transmitting node to this receiver according to a nearest-distance association policy. All other simultaneously transmitting nodes sharing the same time-frequency resources, regardless of whether they are located on the same or different paths, are treated as interfering nodes. This abstraction enables tractable interference and coverage analysis while capturing essential spatial characteristics of real-world CAV networks.

The network of roads, represented by paths P, is modeled as a motion-invariant PLP $\varphi_{\hat{p}}$ with path density $\varrho_{\hat{p}}$. Along each road, vehicular and infrastructure nodes are distributed according to a 1D-PPP with density σ, representing the random spatial locations of nodes constrained to roadways. The superposition of vehicles, roadside units (RSUs), pedestrians, and mobile devices is modeled as independent PPPs with total node intensity $\sigma_n = \sigma_v + \sigma_p + \sigma_R + \sigma_m$. All nodes operate on the same carrier frequency f_c, transmit independently with probability $\mathbb{P}_r$, and use identical transmit power $\wp_w$ and bandwidth B. Accordingly, the set of transmitting nodes on each road is obtained by thinning the original 1D-PPP with density $\sigma_s = \mathbb{P}_r\sigma$, while receiving nodes form an independent thinned PPP with density $\sigma_r = (1 - \mathbb{P}_r)\sigma$. The resulting transmitting and receiving node processes are denoted by φ_s and φ_r, respectively, forming a Poisson line Cox point process.

As shown in Figure 2, the coordinate system is translated such that the tagged receiver is located at the origin of the representation space $\mathcal{S}$. This transformation yields a PLP $\varphi_{\hat{p}_0} = \varphi_{\hat{p}} \cup \{P_0\}$, where P_0 denotes the road passing through the origin. Using Campbell's theorem [10], conditioning on the presence of the tagged receiver is achieved. Each line in the PLP can be uniquely represented by a point (d_i, α_i), where d_i denotes the perpendicular distance from the origin to the line and α_i represents the counterclockwise angle between the line and the x-axis. The number of lines intersecting a disk of radius d follows a Poisson distribution with mean $2\pi\varrho_{\hat{p}}d$.

The objective of this modeling framework is to analyze the coverage probability based on the signal-to-interference ratio (SIR) experienced by the tagged receiver. Specifically, we aim to compute the service probability that the receiver successfully connects to its nearest transmitting node when the received SIR exceeds a predefined threshold Δ.

TABLE 2 | Glossary of notations.

Notation	Description
$\varphi_{\hat{p}}$	Poisson line process representing road paths in the vehicular network.
ψ	Poisson point process modeling the spatial distribution of vehicles or nodes.
R	Euclidean distance between an arbitrary recipient and its closest transmitting node.
$\sigma_{\hat{p}}$	Line density of the Poisson line process (PLP).
$\varrho_{\hat{p}}$	Communication path density of the PLP (equivalent PPP representation).
ϱ_s	Density of source nodes (nodes capable of transmitting signals).
ϱ_r	Density of receiving nodes (nodes capable of receiving signals).
σ_n	Total node density, including vehicles, infrastructure units, and mobile devices.
ν_0	Arbitrary targeted receiver node in the network.
P^s	Coverage probability or link success probability.
$\mathbb{P}$	Probability of an event in stochastic modeling.
Δ	SINR threshold for successful communication.
X_i	Distance of the i-th closest line (path) from the origin in the Poisson line process.
ϵ_i	Event of the serving node being located on line i.

5 | Proposed Solution to C-V2X Interference and Coverage Analysis

To ensure the safe and effective operation of connected and autonomous vehicles, we present stochastic geometry-based interference mitigation among connected vehicles to analyze the performance of vehicular environments. To facilitate our analysis and discussion, we provide an overview of the notation used in this section in Table 2. In the following, we outline the steps involved in the analysis and discussion of interference mitigation in CAVs as depicted in Figure 3.

Step 1: The input distance (R) represents the spatial distance between the vehicles or between a vehicle and infrastructure units.

Step 2 : This step involves specifying the parameters related to the CAVs such as line or path density $\varrho_{\hat{p}}$, source node density ϱ_s, and receiving node density ϱ_r which are essential for modeling the CAVs. The path density represents the density of vehicles on the road. Source node density represents the density of nodes capable of transmitting the signals into the network, including a base station, RSU, or vehicles. Receiving node density refers to the density of nodes that are capable of receiving the signals in the V2X communications.

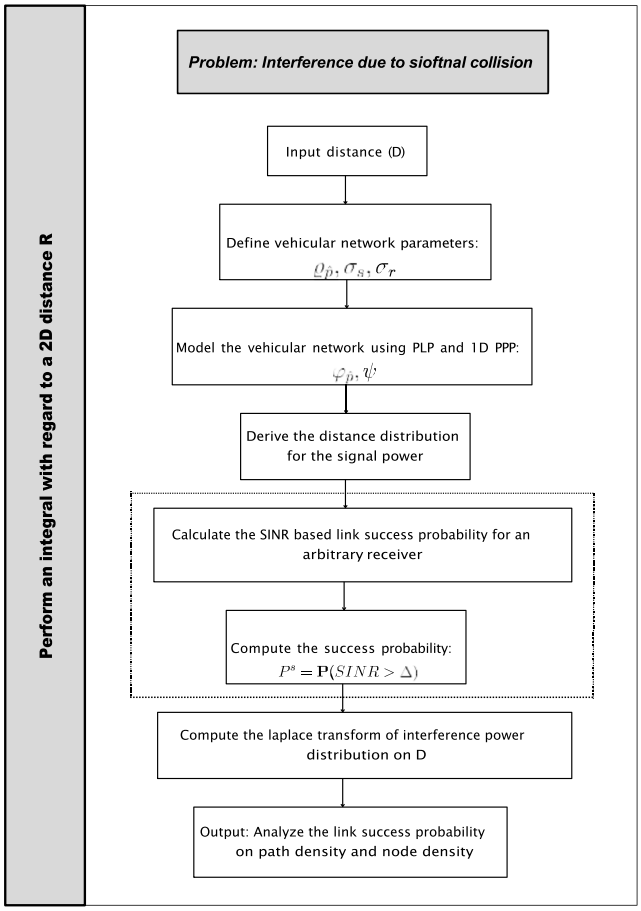

FIGURE 3 | Flowchart of interference mitigation among connected and autonomous vehicles using stochastic geometry.

Step 3: In our model, the roadways are represented using a Poisson line process $\varphi_{\hat{p}}$, which characterizes the random distribution of lines or paths in the region. The positions of nodes on each path are represented using 1D Poisson point process ψ, which is a mathematical model used to represent the random distribution of points (i.e., vehicles or infrastructure units) along the one-dimensional space of each path.

Step 4: We derive the distance D between the recipient and the source node. This distance characterization helps to understand the spatial relationship between CAVs and the infrastructure, enabling us to analyze interference patterns and signal propagation characteristics.

Step 5-7 : The assessment of wireless communication quality in CAVs involves calculating the SINR at the recipient node. The shared nature of the wireless medium in CAVs makes it a crucial performance metric, that quantifies the likelihood of achieving reliable and error-free communication. Our system model employs Nakagami-m fading model [10] to characterize the wireless channel variability caused by multipath propaga-

tion and shadowing effects. This versatile fading model offers analytical traceability as compared to the Rayleigh fading model.

The fading gain for the interfering link from the k^{th} source node is denoted as C_{vP_k} and follows the Nakagami distribution with shape parameter m, which controls the severity of fading, and scale parameter Ω, which controls the fading spread. Specifically, it is represented as $C_{v_{P_k}} \sim \text{Nakagami}(m, \Omega)$, where $C_{v_{P_k}}$ denotes the fading gain of the interfering link.

We assume a nearest-node association policy for the arbitrary recipient. This association rule is equivalent to the strongest-signal association under the assumptions of homogeneous transmit power, identical antenna heights, and omnidirectional antenna patterns across vehicles, RSUs, and base stations, which is standard in stochastic-geometry-based vehicular network analysis.

Then, the SINR at the arbitrary (tagged) receiver is given by,

$$\text{SINR} = \frac{C_0 D^{-\beta}}{\sum_{P_k \in \varphi_{\hat{p}_0}} \sum_{\mathbf{v}_{P_k} \in \psi_{P_k} \setminus \hat{c}(0,D)} C_{\mathbf{v}_{P_k}} \|\mathbf{v}_{P_k}\|^{-\beta} + \mathcal{N}}, \tag{2}$$

where C_0 denotes the Nakagami-m fading gain of the desired link between the tagged receiver and its nearest transmitting node, and D is the Euclidean distance between them. The parameter $\beta > 2$ represents the path-loss exponent. The set $\varphi_{\hat{p}_0}$ denotes the PLP of all road segments after conditioning on the presence of the tagged receiver, including the typical road P_0 passing through the origin. For each road $P_k \in \varphi_{\hat{p}_0}$, the set ψ_{P_k} represents the 1D-PPP of simultaneously transmitting nodes located on that road. A point $\mathbf{v}_{P_k} \in \psi_{P_k}$ denotes the location of an interfering transmitter on road P_k, and $\|\mathbf{v}_{P_k}\|$ is its Euclidean distance from the tagged receiver. The exclusion region $\hat{c}(0, D) = \{\mathbf{x} \in \mathbb{R}^2 : \|\mathbf{x}\| \leq D\}$ ensures nearest-transmitter association by excluding all other transmitters closer than the serving node. $\mathcal{N}$ denotes the receiver noise power.

After calculating the SINR, the link success probability of CAVs is computed when they establish connections with other CAVs or RSUs located on the same PLP. The success probability evaluates the probability that SINR at the recipient exceeds a certain threshold as computed below.

$$\begin{aligned} P^s &= \mathbf{P}(SINR > \Delta) \\ &= \sum_{j=0}^{\infty} \mathbf{P}(\epsilon_j)\mathbf{P}(SINR > \Delta|\epsilon_j) \end{aligned} \tag{3}$$

It is noted that P^s represents the spatially averaged link success probability obtained by averaging over random network realizations, while the explicit probability distribution of the success rate across individual realizations is beyond the scope of this work.

$$\begin{aligned} P^s &= \mathbf{P}(\epsilon_0)\mathbf{P}(SINR > \Delta|\epsilon_0) \\ &+ \sum_{n=1}^{\infty} \mathbb{E}_{W_n}[\mathbf{P}(\epsilon_n|W_n)\mathbf{P}(SINR > \Delta|\epsilon_n, W_n)] \end{aligned} \tag{4}$$

$$\begin{aligned} P^s = \mathbf{P}(\epsilon_0) &\sum_{r=0}^{m-1} \int_0^{\infty} \frac{(-m\Delta)^r}{d^{-r\beta} r!} \times \left[\frac{\partial^r}{\partial u^r} \mathfrak{L}_I(u|d, \epsilon_0)\right]_{s=m\Delta r^{\alpha}} f_D(d|\epsilon_0) dd \\ &+ \sum_{n=1}^{\infty} \sum_{r=0}^{m-1} \int_0^{\infty} \int_{w_n}^{\infty} \frac{(-m\Delta)^r}{d^{-r\alpha} r!} \\ &\times \left[\frac{\partial^r}{\partial u^r} \mathfrak{L}_I(u|d, \epsilon_0, w_n)\right]_{w=m\Delta d^{\beta}} \\ &\times \mathbf{P}(\epsilon_n|W_n) f_D(d|\epsilon_n, W_n) f_{W_n}(w_n) dr\, dw_n \end{aligned} \tag{5}$$

where, $f_D(d|\epsilon_n, W_n)$ is the nearest node distribution, calculated as,

$$\begin{aligned} F_D(d) &= 1 - \mathbb{P}(D > d) \\ &= 1 - \mathbb{P}(\mathbb{N}(\hat{c}(0, d)) = 0) \\ &= 1 - exp\left(-2\varrho_v d - 2\pi\varrho_p\right) \\ &\times \left[\int_0^d \left(1 - exp\left(-2\varrho\sqrt{d^2 - w^2}\right)\right) dd\right] \end{aligned} \tag{6}$$

The link success probability, denoted as P^s is computed using Equation (3), for various interference events ϵ_i, and their respective probabilities. This equation is further expanded into Equations (4) and (5), which involve the computation of the Laplace transform of the interference power distribution for each interference event. It represents the probability of encountering an interference event ϵ_0 due to signal collision and the conditional probability of achieving a higher SINR than Δ in that particular event. Equation (6), defines the nearest node distribution between the receiver and the closest transmitting node, where $\mathbb{N}$ denotes that there is no node along the paths intersecting the disk. Thus, these equations specify the success probability of achieving reliable and error-free communication at the arbitrary receiver (or user) denoted as u on the same PLP. This arbitrary receiver u is randomly chosen from the set of receivers located on the PLP which connects to the nearest node on the particular path without interference.

Step 8 : In the final step, we analyze the link success probability on the path density and communication node density. The link success probability of a arbitrary recipient worsens as the path density increases. If the communication node density increases, the link success probability of a arbitrary recipient improves which is analyzed and discussed in the subsequent section. For low path density and moderate node density, the link success probability is represented by Equation (5):

$$\begin{aligned} P^c = &\sum_{r=0}^{m-1} \int_0^{\infty} \frac{(-m\Delta d^{\beta})^r}{r!} \frac{\partial^r}{\partial s^r} \\ &\times \left[\exp\left(-2\varrho_v \int_d^{\infty} \left(1 - \left(1 + \frac{sy^{-\beta}}{m}\right)^{-m}\right)\right.\right. \\ &\left.\left. \times\, y\, dy\right)\right] 2\varrho_s \exp(-2\varrho_s d)\, dd \end{aligned} \tag{7}$$

For high line density and low node density, the coverage probability is represented by Equation (6):

$$P^c = \sum_{r=0}^{m-1} \int_0^{\infty} \frac{(-m\Delta d^{\beta})^r}{r!} \frac{\partial^r}{\partial s^r} \times \left[exp(-2\pi\varrho_{\hat{p}}\varrho_{\upsilon} \int_d^{\infty} \left(1 - \left(1 + \frac{sy^{-}\beta}{m}\right)^{-m}\right) \times y\, dy \right) \right] 2\pi\varrho_{\hat{p}}\varrho_{\upsilon} exp(-\sigma_{\hat{p}}\varrho_s \pi d^2) dr \quad (8)$$

Therefore, the stochastic geometry model provides an analytical framework to study the impact of interference caused by signal collisions among CAVs as a function of communication node density and path density parameters. By incorporating SINR requirements of different CAV communication links, the framework facilitates a systematic evaluation of how network parameters influence spatial coverage and link success probability. The quantitative performance implications and design insights derived from this model are presented and discussed in the subsequent simulation and results sections.

Algorithm 1 summarizes the analytical workflow of the proposed stochastic geometry-based interference and coverage analysis. The algorithm outlines the sequence of modeling, interference characterization, and spatial averaging steps used to derive the closed-form expressions for SINR and link success probability.

ALGORITHM 1 | Stochastic Geometry-Based Interference and Coverage Analysis for C-V2X Networks

Require: Path density $\varrho_{\hat{p}}$, source node density σ_s, receiver density σ_r, path-loss exponent β, SINR threshold Δ, Nakagami-m fading parameters (m, Ω), noise power $\mathcal{N}$

Ensure: Spatially averaged link success probability P^s for an arbitrary receiver

1: Model the road topology using a Poisson Line Process (PLP) $\varphi_{\hat{p}}$

2: Model transmitting and receiving nodes on each road using 1D Poisson Point Processes (PPP) ψ

3: Place an arbitrary receiver ν_0 at the origin using Slivnyak's theorem

4: Associate ν_0 with its nearest transmitting node at distance D

5: Derive the probability density function $f_D(d)$ of the serving distance D

6: Model small-scale fading for desired and interfering links using Nakagami-m distribution

7: Characterize aggregate interference from all transmitting nodes on $\varphi_{\hat{p}_0}$

8: Compute the Laplace transform of interference $\mathcal{L}_I(\cdot)$

9: Evaluate the SINR at the arbitrary receiver:

$$\text{SINR} = \frac{C_0 D^{-\beta}}{I + \mathcal{N}}$$

10: Compute the conditional success probability $\mathbb{P}(\text{SINR} > \Delta \mid D)$

11: Average over spatial realizations of D and interference to obtain:

$$P^s = \mathbb{P}(\text{SINR} > \Delta)$$

12: Analyze the impact of path density $\varrho_{\hat{p}}$ and node density σ_s on P^s

13: **return** Spatially averaged link success probability P^s

6 | Simulations Environment

6.1 | Simulation Setup

In this section, we evaluate the performance of our model and analyze the trends in link success probability under various communication path density and node density scenarios, aiming to optimize the successful transmission of V2X communications. To validate the accuracy of our proposed theoretical analysis, we conduct MATLAB simulations. Our study involves a CAVs setup, where vehicles are deployed along roads following a PPP. We randomly select a transmitter whose average transmission range covers the test receiver located at the origin. Throughout the simulations, we assume that all vehicles utilize the CSMA MAC protocol. The CSMA is employed for numerical validation and is not analytically coupled to the proposed stochastic geometry-based framework. The selected simulation parameters include a path-loss exponent $\beta = 4$, a communication path density $\varrho_{\hat{p}} = 30$ km/km^2, and a vehicle density $\sigma_n = 30$ nodes/km, along with infrastructure units. Table 3 summarizes the simulation parameters which are selected to reflect realistic scenarios encountered in urban, suburban, and rural environments, ensuring the generalizability of the results.

It is important to note that vehicle mobility and speed are not accounted for within the simulation. The simulation assumes a snapshot view of the vehicular network based on a random distribution of the vehicles distributed along roads according to Poisson point processes. This assumption is based on a snapshot view of a point process in stochastic geometry. This snapshot-based assumption is commonly adopted in stochastic geometry-based studies, as the instantaneous SINR and link success probability primarily depend on spatial configurations rather than vehicle speed.

The use of stochastic geometry ensures that the results are robust and adaptable to a wide range of vehicular network configurations, including variations in traffic density, infrastructure deployments, and fading conditions. In the following section, we explore the impact of these parameters on the probability of achieving successful data transmission and discuss the validity and generalizability of our findings.

TABLE 3 | Experimental settings for simulation.

Parameter	Value/description
Path-loss exponent (β)	4 (urban environment)
Communication path density ($\varrho_{\hat{p}}$)	30 km/km^2 (varied from 10 to 60)
Node density (σ_n)	30 nodes/km (varied from 10 to 60)
Fading model	Nakagami-m (varying m values from 0.5 to 3.5)
Traffic density	Varying between 10 and 50 nodes/km
Simulation area	2D plane representing road network
Frequency (f_c)	Constant (same frequency for all vehicles)
MAC protocol	CSMA (carrier sense multiple access)
SINR threshold	Varying threshold to analyze success probability
Simulation tool	MATLAB
Simulation scenarios	Varying path densities, node densities, and fading models

6.2 | Performance Evaluation

We have evaluated the performance of our proposed model by formulating multiple scenarios to compute the link success probability and SINR for an arbitrary receiver for successful communication in V2X communications networks. In this section, we present the simulation analysis, highlighting how various parameters influence the performance of the V2X communications network.

6.2.1 | Impact of Communication Path Density on Link Success Probability

As shown in Figure 4, we first evaluate the probability of successful transmission at the arbitrary receiver with varying communication path/road densities $\varrho_{\hat{p}} = 10$, 20, 30, 40, and 50 km/km^2 as a function of SINR threshold. We consider the node density σ_n here to be 30 nodes/km. It can be observed from Figures 4a and 4b, that as the communication path density increases, the link success probability tends to decrease.

The increase in path density causes the lines to come closer, however, the distance between the source vehicle and the arbitrary receiver remains the same. As a result, the desired signal power remains constant, while the interference power from other nodes increases due to the closer proximity of interfering nodes to the receiver. This results in a decline in the link success probability.

These findings are consistent with theoretical expectations since higher path densities bring interfering nodes closer to the receiver, thereby increasing interference and reducing the SINR. This trend is applicable across varying road network layouts, from sparsely connected highways to densely packed urban grids. The results are validated under different path densities, representing realistic vehicular traffic scenarios. This ensures their generalizability to diverse deployment conditions, such as dense urban areas or rural highways with sparse road networks.

6.2.2 | Effect of Node Density on Link Success Probability

In the next scenario, we examine the link success probability of the arbitrary receiver for different node densities $\sigma_n = 10$, 20, 30, 40, and 50 nodes/km as a function of the SINR threshold. As illustrated in Figure 5a, the link success probability demonstrates an increasing trend with higher node density. The closer proximity of vehicular and infrastructure nodes reduces the distance between the source and the receiver, which results in increased desired signal power for communication. While the interfering nodes also come closer, they are not positioned along the path connecting the arbitrary receiver. As a result, the probability of successful transmission of signals rises with the increase in node density. In Figure 5b, the success probability is shown as a function of SINR threshold for different node densities, demonstrating that higher node densities maintain higher success probabilities even as the SINR threshold increases.

The observed trends align with real-world scenarios where increased node density enhances the likelihood of reliable communication due to shorter transmitter-receiver distances. This is particularly relevant in those cases where large densities of connected vehicles or infrastructure nodes exist, such as cities with many RSUs. The results would be generally applicable to networks with a wide range of node densities in all areas, from very sparse rural settings to highly dense urban settings.

6.2.3 | Impact of Path-Loss Exponent on Link Success Probability and Spectral Efficiency

Figure 6b illustrates the impact of various path-loss exponents $\beta = 2$, 2.5, 3, 3.5, and 4 on link success probability and spectral efficiency. Figure 6a illustrates that the success probability diminishes as the path-loss exponent increases, attributable to the swift attenuation of signal strength. As β increases, the impact of distance on signal attenuation becomes more pronounced, reducing the likelihood of successful transmission. Figure 6b shows the spectral efficiency as a function of traffic density for various path densities. It can be observed that higher traffic densities and path densities lead to an increase in spectral efficiency, highlighting the potential for enhanced network performance in dense traffic conditions. This observation highlights a fundamental reliability-throughput tradeoff in V2X communications networks. At lower traffic densities, reduced interference leads to higher instantaneous SINR values, which improves spectral efficiency. However, lower node density also increases transmitter-receiver separation and reduces spatial reuse, thereby decreasing the probability of successful link establishment. Conversely, higher traffic densities enhance connectivity and link success probability at the cost of increased interference and reduced spectral efficiency.

Path-loss exponents are chosen to represent realistic wireless propagation environments, such as free space ($\beta = 2$) or urban

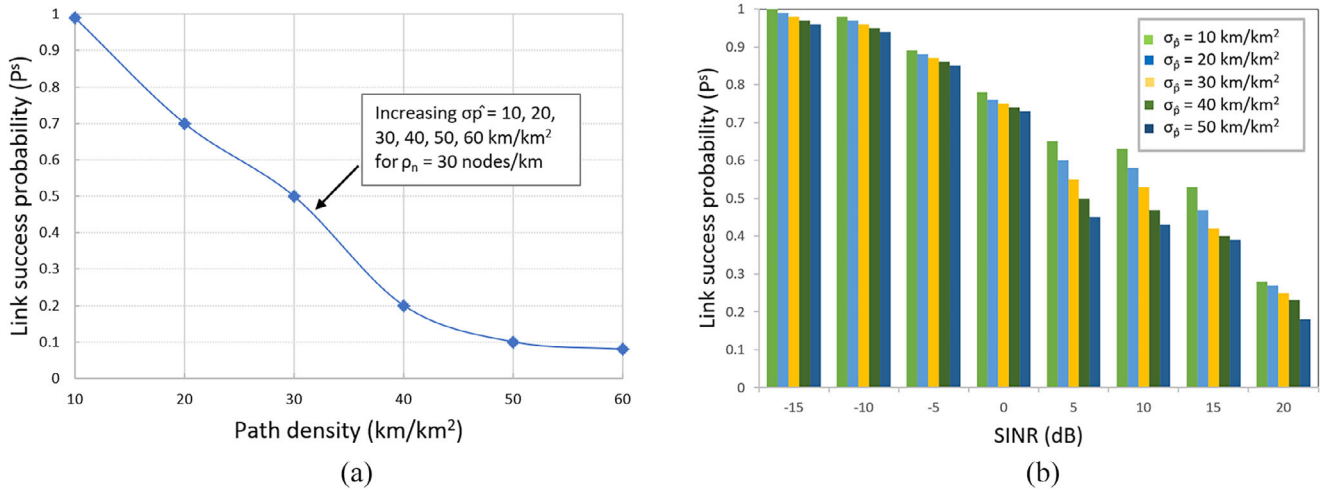

FIGURE 4 | Link success probability using poisson point process theory. (a) Success probability as a function of increasing path density (km/km^2). (b) Success probability of the arbitrary receiver as a function of SINR threshold for different path densities.

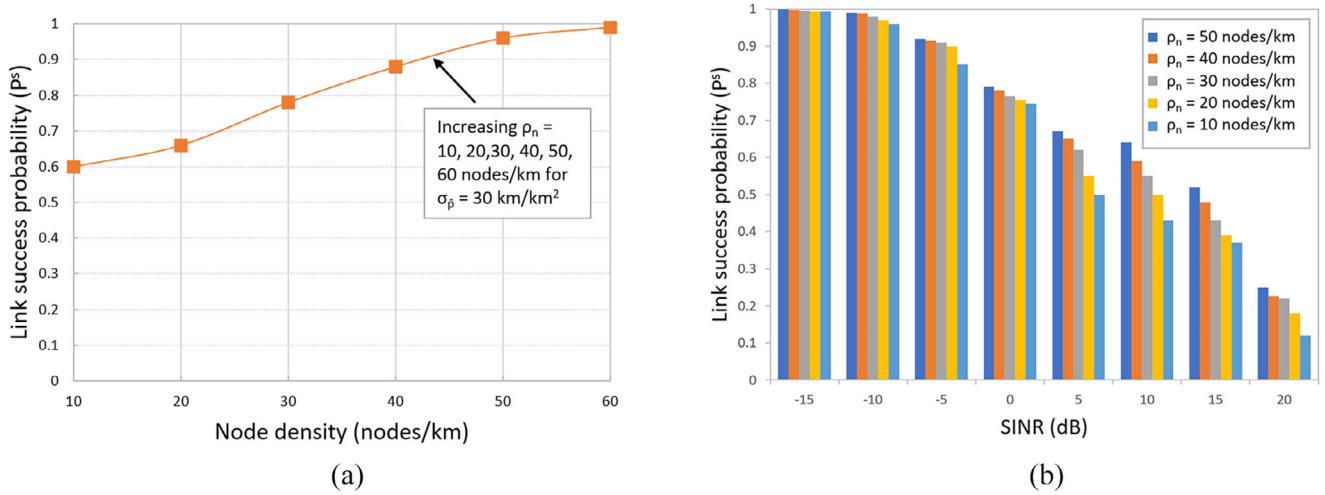

FIGURE 5 | Link success probability using poisson point process theory: (a) Success probability as a function of increasing node density (nodes/km). (b) Success probability of the arbitrary receiver as a function of SINR threshold for different node densities.

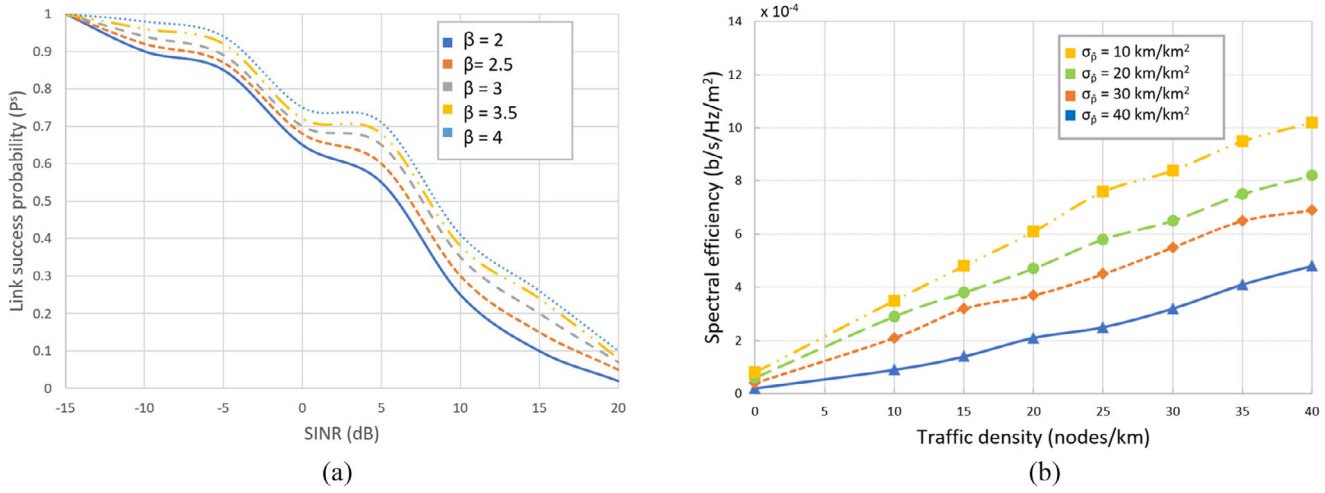

FIGURE 6 | Link success probability analysis for an arbitrary receiver: (a) Success probability as a function of SINR threshold for different path-loss exponents. (b) Spectral efficiency as a function of traffic density.

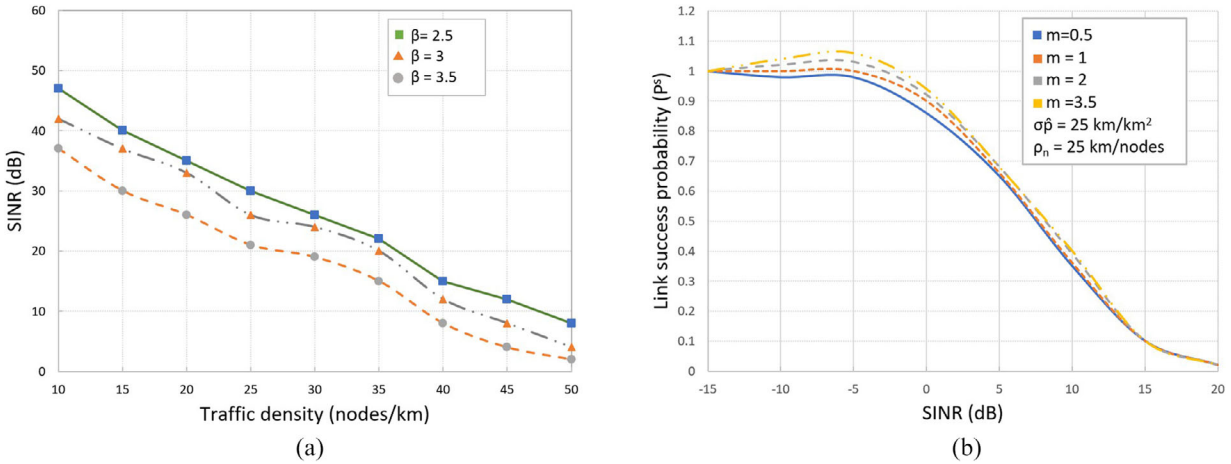

FIGURE 7 | (a) SINR as a function of traffic density for different path-loss exponents. (b) Link success probability as a function of SINR threshold for different Nakagami-m fading parameters.

environments with significant signal obstruction ($\beta \geq 3$). This ensures that the findings are valid for a wide range of deployment scenarios. The spectral efficiency trends reflect the scalability of the model for dense traffic environments, where efficient resource utilization is critical.

6.2.4 | Analysis of SINR and Success Probability Under Nakagami-m Fading

Figure 7 demonstrates the analysis of SINR and success probability under different Nakagami-m fading parameters $m = 0.5, 1, 2, 3.5$. Figure 7a illustrates the variation of SINR with traffic density for different path-loss exponents. It is observed that SINR decreases as traffic density increases due to higher interference levels. Figure 7b illustrates the link success probability as a function of SINR for different Nakagami-m fading parameters. The higher values of m indicate less severe fading, resulting in improved communication reliability and higher success probabilities.

The use of Nakagami-m fading ensures the robustness of the results under diverse fading conditions, from severe fading in urban canyons ($m = 0.5$) to mild fading in open environments ($m \geq 2$). These results generalize to environments that exhibit wide variability in the channel conditions, ensuring applicability for whole sets of real-world vehicular communication scenarios.

Thus, the simulation analysis validates that our proposed model is very effective in characterization and analysis of performance related to V2X communications networks under differing scenarios. Insights from this work are valuable for the design of robust and efficient communication strategies in order to deploy connected and autonomous vehicles in intelligent transportation systems.

7 | Comparison With Existing Solutions

In this section, we provide a comparison of the computational efficiency, memory, and communication overhead of our approach compared to the existing approaches, that is, agent-based models [30], geolocation-based communication (GLOC) [11], and grid-based models [31].

The agent-based models represent individual agents (CAVs or infrastructure units) and their interaction using the discrete-event simulation approach. While agent-based models assure a high degree of realism, these models suffer from high computational complexity because each vehicle's behaviour, communication, and interaction need to be simulated in real time. The GLOC model optimizes communication using vehicle locations and geolocation-based information to ensure efficient communication. These models also suffer from high communication overhead as they are derived from location information exchanges, increasing the system's complexity when the network becomes large. Furthermore, the grid-based models divide the simulation region into a grid and study the interactions of the vehicles based on grid cell-based relationships. These models are often memory-intensive to manage the grid structure in large-scale environments like urban locations and are computationally intensive where the number of grid cells is large.

Table 4 illustrates the comparative performance of the proposed stochastic geometry-based model with respect to the existing approaches, with key parameters such as computational complexity, memory usage, communication overhead, accuracy, and scalability in the V2X communications networks. The complexity values depicted in Table 4 are derived analytically from the mathematical structure of the proposed stochastic geometry framework rather than from empirical runtime measurements. The proposed framework evaluates interference and link success probability using closed-form expressions derived from the probability generating functional (PGFL) and Laplace transform of Poisson point processes [7], which avoids explicit pairwise interactions among nodes and results in linear complexity $\mathcal{O}(N)$ with respect to node density.

7.1 | Computational Complexity

The stochastic geometry-based approach presented in this study leverages PLP and PPP to model road layouts and node

TABLE 4 | Comparison of the proposed framework with existing solutions.

Feature	Proposed framework	Agent-based models [30]	GLOC [11]	Grid-based models [31]
Computational complexity	$\mathcal{O}(N)$	$\mathcal{O}(N^2)$	$\mathcal{O}(N\log(N))$	$\mathcal{O}(N^2)$
Memory usage	$\mathcal{O}(P+N)$	$\mathcal{O}(N\times P)$	$\mathcal{O}(N\times P)$	$\mathcal{O}(N\times P)$
Communication overhead	$\mathcal{O}(N)$	$\mathcal{O}(N^2)$	$\mathcal{O}(N\log(N))$	$\mathcal{O}(N^2)$
Accuracy	High (Nakagami-m)	Medium (parameter dependent)	High	Medium
Scalability	High (due to PLP/PPP)	Limited	Medium	Limited

distributions. This offers a significant computational advantage compared to grid-based and agent-based simulation frameworks. Grid-based models [31] require $\mathcal{O}(N^2)$ complexity to account for pairwise interactions among N vehicles, especially for interference analysis, whereas our framework reduces this to $\mathcal{O}(N)$ due to the mathematical tractability of the Poisson process.

In interference analysis, the derivation of SINR and link success probability in our model leverages the Laplace transform of interference distributions, which simplifies the evaluation to $\mathcal{O}(\log(N))$ for N interfering nodes per unit area. Traditional geometric models that simulate interference directly often have complexity $\mathcal{O}(N^2)$ or higher, especially in dense urban environments with overlapping coverage areas.

7.2 | Memory Space Complexity

Agent-based models often require significant memory to store the states of vehicles, paths, and their interactions, typically scaling with $\mathcal{O}(N\times P)$ where N is the number of vehicles and P is the number of paths [30]. Our approach simplifies this by representing the roads using PLP and vehicles using PPP, which reduces memory requirements to $\mathcal{O}(P+N)$. Additionally, the use of thinning operations in PPP (e.g., for separating source and receiving nodes) avoids the need for additional state-tracking variables, further optimizing memory usage.

7.3 | Communication Complexity

In vehicular networks, efficient communication is crucial to maintaining low latency and high reliability. The GLOC model [11] and similar geolocation-based approaches often involve significant overhead for transmitting and receiving location data, resulting in a communication complexity proportional to $\mathcal{O}(N\log(N))$ for coordination among N nodes. In contrast, our stochastic geometry framework calculates spatial relationships and interference distributions probabilistically, reducing the communication complexity to $\mathcal{O}(N)$ by avoiding explicit coordination among vehicles.

Additionally, the proposed model's reliance on Nakagami-m fading ensures accurate representation of channel variability without introducing iterative recalculations for fading conditions, which further reduces communication overhead compared to models that rely on dynamic path-loss recalibration.

7.4 | Accuracy vs. Complexity Tradeoff

While simpler statistical models, such as Rayleigh fading, provide lower computational complexity for SINR calculations, they often fail to capture real-world fading behaviors in urban vehicular networks. In this work, Nakagami-m fading is employed solely as a channel modeling assumption within the proposed stochastic geometry framework to represent a wide range of propagation conditions. Although this choice introduces slightly higher computational overhead compared to Rayleigh fading, it enables a more realistic characterization of channel variability and interference effects. Here, accuracy refers to the fidelity of channel and interference modeling achieved by the proposed PLP-PPP-based analytical framework, rather than to empirical or learning- based on prediction accuracy. The balance between modeling fidelity and analytical tractability ensures that the framework remains both practical and reliable for performance evaluation of C-V2X communications networks.

8 | Conclusion, Limitation, and Future Work

A comprehensive analytical framework for modeling the communication of connected and autonomous vehicles (CAVs) is presented, based on stochastic geometry and Poisson process theory. The roads are modeled as pathways using the PLP, while the traffic entities (vehicles and infrastructure units) are represented as a homogeneous 1D PPP. The expressions for SINR and link success probability for an arbitrary receiver connecting to its nearest transmitting node, assuming Nakagami-m fading, have been obtained. We computed these expressions to assess the interference at the arbitrary receiver and to study the trends in the probability of successful data transmission for varying pathways and traffic density. The analytical findings are quantitatively validated by comparison with simulations that are executed in MATLAB. The results of the simulations provide insightful information in the design and application of connected and autonomous vehicles (CAVs).

However, this work provides valuable insights, some limitations should be acknowledged in the current framework. First, the model relies on a homogeneous distribution of vehicles and infrastructure nodes, which fails to capture the real-world dynamic and clustered traffic patterns in urban areas. Second, the Nakagami-m fading model employed to model channel conditions is unlikely to accurately account for all environmental factors, including line-of-sight (LOS) blockages and urban canyon effects that can impact communication reliability. Moreover,

the proposed analysis relies on a static spatial snapshot of the vehicular network. Although this assumption has been adopted in many stochastic geometry-based studies for ease of enabling tractable analytical characterization, it does not capture explicitly the mobility of vehicles, Doppler effects, or any kind of temporal correlation of interference across consecutive transmission slots. The framework thus focuses on instantaneous spatial reliability rather than time-correlated performance metrics, such as the reliability of periodic safety beacons. Important directions for future extension of the presented framework to time-evolving C-V2X communications scenarios shall consider point processes that are aware of node mobility, as well as temporally correlated models of interference.

For future research, the framework can be extended to simulate urban traffic scenarios at intersections where traffic is constrained to designated lanes, including traffic lights, pedestrians, and emergency vehicles. In addition, the application of Ricean fading models is expected to enhance the reliability of assessments of CAV communication, particularly in scenarios with dominant line-of-sight (LOS) channels as well as dispersed signals, thus reflecting a more realistic model of communication. Moreover, the deployment of fifth-generation (5G) as well as sixth-generation (6G) wireless communication technologies is expected to provide low-latency, high-reliability, and widespread connectivity to CAVs, thus optimizing their functional efficiency in dynamic environments.

Author Contributions

A. M. A. and A. B. contributed to the conceptualisation of the study, methodology, data curation, interpretation of results, and manuscript writing. X. C. provided overall supervision, funding and guidance throughout the research process. All authors reviewed and approved the final manuscript.

Acknowledgements

This work was supported by UKRI EPSRC Grant funded Doctoral Training Centre at Swansea University, through PhD Project RS718 on Explainable AI. The authors also have been supported by UKRI EPSRC Grant EP/W020408/1 Project SPRITE+ 2: The Security, Privacy, Identity and Trust Engagement Network Plus (phase 2).

Funding

The authors have been funded by UKRI EPSRC Grant EP/W020408/1 Project SPRITE+ 2: The Security, Privacy, Identity and Trust Engagement Network Plus (phase 2) for this study. The authors also have been funded by PhD Project RS718 on Explainable AI through UKRI EPSRC Grant funded Doctoral Training Centre at Swansea University.

Conflicts of Interest

The authors declare no conflicts of interest.

Data Availability Statement

Data will be available upon request.

References

1. P. Papadimitratos, A. De La Fortelle, K. Evenssen, R. Brignolo, and S. Cosenza, "Vehicular Communication Systems: Enabling Technologies, Applications, and Future Outlook on Intelligent transportation," *IEEE Communications Magazine* 47, no. 11 (2009): 84–95.

2. X. Gu, B. Leng, L. Zhang, J. Miao, and L. Zhang, "A Stochastic Geometry Approach to Model and Analyze Future Vehicular Communication Networks," *IEEE Access* 8 (2020): 14500–14512.

3. S. Zeadally, M. A. Javed, and E. B. Hamida, "Vehicular Communications for ITS: Standardization and Challenges," *IEEE Communications Standards Magazine* 4, no. 1 (2020): 11–17.

4. L. Ye and T. Yamamoto, "Modeling Connected and Autonomous Vehicles in Heterogeneous Traffic Flow," *Physica A: Statistical Mechanics and Its Applications* 490 (2018): 269–277.

5. A. Nikitas, A.-E. Vitel, and C. Cotet, "Autonomous Vehicles and Employment: An Urban Futures Revolution or Catastrophe?" *Cities* 114 (2021): 103203.

6. K. Wevers and M. Lu, "V2X Communication for ITS: From IEEE 802.11 p Towards 5G," *IEEE 5G Tech Focus* 1, no. 2 (2017): 5–10.

7. A. Al-Hourani, R. J. Evans, S. Kandeepan, B. Moran, and H. Eltom, "Stochastic Geometry Methods for Modeling Automotive Radar Interference," *IEEE Transactions on Intelligent Transportation Systems* 19, no. 2 (2017): 333–344.

8. M. J. Farooq, H. ElSawy, and M.-S. Alouini, "A Stochastic Geometry Model for Multi-Hop Highway Vehicular Communication," *IEEE Transactions on Wireless Communications* 15, no. 3 (2015): 2276–2291.

9. L. Cheng, B. E. Henty, D. D. Stancil, F. Bai, and P. Mudalige, "Mobile Vehicle-to-Vehicle Narrow-Band Channel Measurement and Characterization of the 5.9 GHz Dedicated Short Range Communication (DSRC) Frequency Band," *IEEE Journal on Selected Areas in Communications* 25, no. 8 (2007): 1501–1516.

10. H. ElSawy, A. Sultan-Salem, M.-S. Alouini, and M. Z. Win, "Modeling and Analysis of Cellular Networks Using Stochastic Geometry: A Tutorial," *IEEE Communications Surveys & Tutorials* 19, no. 1 (2016): 167–203.

11. F. J. Martin-Vega, B. Soret, M. C. Aguayo-Torres, I. Z. Kovacs, and G. Gomez, "Geolocation-Based Access for Vehicular Communications: Analysis and Optimization via Stochastic Geometry," *IEEE Transactions on Vehicular Technology* 67, no. 4 (2017): 3069–3084.

12. Z. Qin, A. Ji, Z. Sun, G. Wu, P. Hao, and X. Liao, "Game Theoretic Application to Intersection Management: A Literature Review," *IEEE Transactions on Intelligent Vehicles* 10, no. 4 (2024): 2589–2607.

13. S. Fang, P. Hang, C. Wei, Y. Xing, and J. Sun, "Cooperative Driving of Connected Autonomous Vehicles in Heterogeneous Mixed Traffic: A Game Theoretic Approach," *IEEE Transactions on Intelligent Vehicles* (2024).

14. S. Karimi, A. Karimi, and A. Vahidi, "Level-k Reasoning, Deep Reinforcement Learning, and Monte Carlo Decision Process for Fast and Safe Automated Lane Change and Speed Management," *IEEE Transactions on Intelligent Vehicles* 8, no. 6 (2023): 3556–3571.

15. C.-S. Choi and F. Baccelli, "A Stochastic Geometry Model for Spatially Correlated Blockage in Vehicular Networks," *IEEE Internet of Things Journal* 9, no. 20 (2022): 19881–19889.

16. T. Zeng, O. Semiari, M. Chen, W. Saad, and M. Bennis, "Federated Learning on the Road Autonomous Controller Design for Connected and Autonomous Vehicles," *IEEE Transactions on Wireless Communications* 21, no. 12 (2022): 10407–10423.

17. P. R. Verma, N. P. Singh, and D. Pantola, "Unleashing the Power of Deep Neural Networks: An Interactive Exploration of Static and Dynamic Architectures," *Multimedia Tools and Applications* 83 (2024): 1–37.

18. B. E. Y. Belmekki, A. Hamza, and B. Escrig, "Cooperative Vehicular Communications at Intersections over Nakagami-m Fading Channels," *Vehicular Communications* 19 (2019): 100165.

19. J. Zhang, X. Guo, Z. Fu, Y. Liu, and Y. Ding, "Non-cooperative game theory based driver-automation shared steering control considering

driver steering behavior characteristics," *IEEE Internet of Things Journal* 11, no. 17 (2024): 28465–28479.

20. Y. Liang, N. Ma, X. Li, and J. Hu, "Stochastic Roadside Unit Location Optimization for Information Propagation in the Internet of Vehicles," *IEEE Internet of Things Journal* 8, no. 17 (2021): 13316–13327.

21. K. Ji, N. Li, M. Orsag, and K. Han, "Hierarchical and Game-Theoretic Decision-Making for Connected and Automated Vehicles in Overtaking Scenarios," *Transportation Research Part C: Emerging Technologies* 150 (2023): 104109.

22. M. Fu, S. Li, M. Guo, et al., "Cooperative Decision-Making of Multiple Autonomous Vehicles in a Connected Mixed Traffic Environment: A Coalition Game-Based Model," *Transportation Research Part C: Emerging Technologies* 157 (2023): 104415.

23. A. M. Aslam, A. Bhardwaj, R. Chaudhary, and I. Budhiraja, "A Cooperative Game Approach for Multi-Lane Merging Decision-Making Algorithm for CAVs," in *Proceedings of the 25th International Conference on Distributed Computing and Networking* (IEEE, 2024), 274–279.

24. D. Hug and M. Reitzner, "Introduction to Stochastic Geometry," *Stochastic Analysis for Poisson Point Processes: Malliavin Calculus, Wiener-Itô Chaos Expansions and Stochastic Geometry* (Springer International Publishing, 2016), 145–184.

25. Y. Hmamouche, M. Benjillali, S. Saoudi, H. Yanikomeroglu, and M. Di Renzo, "New Trends in Stochastic Geometry for Wireless Networks: A Tutorial and Survey," *Proceedings of the IEEE* 109, no. 7 (2021): 1200–1252.

26. M. J. Farooq, H. ElSawy, and M.-S. Alouini, "Modeling Inter-vehicle Communication in Multi-Lane Highways: A Stochastic Geometry Approach," in *2015 IEEE 82nd Vehicular Technology Conference (VTC2015-Fall)* (IEEE, 2015), 1–5.

27. Z. Tong, H. Lu, M. Haenggi, and C. Poellabauer, "A Stochastic Geometry Approach to the Modeling of DSRC for Vehicular Safety Communication," *IEEE Transactions on Intelligent Transportation Systems* 17, no. 5 (2016): 1448–1458.

28. D. Stoyan, W. S. Kendall, S. N. Chiu, and J. Mecke, *Stochastic Geometry and Its Applications* (John Wiley & Sons, 2013).

29. G. A. Safdar, M. Ur-Rehman, M. Muhammad, M. A. Imran, and R. Tafazolli, "Interference Mitigation in D2D Communication Underlaying LTE-A Network," *IEEE Access* 4 (2016): 7967–7987.

30. H. Fujii, H. Uchida, and S. Yoshimura, "Agent-Based Simulation Framework for Mixed Traffic of Cars, Pedestrians and Trams," *Transportation Research Part C: Emerging Technologies* 85 (2017): 234–248.

31. J. Godoy, V. Jiménez, A. Artuñedo, and J. Villagra, "A Grid-Based Framework for Collective Perception in Autonomous Vehicles," *Sensors* 21, no. 3 (2021): 744.